Supplementary material
A sensitivity leap for X-band EPR using a probehead with a cryogenic preamplifier

Mantas Šimėnas,[1, a)] James O'Sullivan,[1] Christoph W. Zollitsch,[1] Oscar Kennedy,[1] Maryam Seif-Eddine,[2] Irina Ritsch,[3] Miriam Hülsmann,[4] Mian Qi,[4] Adelheid Godt,[4] Maxie M. Roessler,[2] Gunnar Jeschke,[3] and John J.L. Morton[1, 5, b)]

[1)] *London Centre for Nanotechnology, University College London, London WC1H 0AH, UK*

[2)] *Department of Chemistry, Imperial College London, Molecular Sciences Research Hub, London W12 0BZ, UK*

[3)] *ETH Zürich, Department of Physical Chemistry, Vladimir-Prelog-Weg 2, 8093 Zürich, Switzerland*

[4)] *Faculty of Chemistry and Center for Molecular Materials (CM2), Bielefeld University, Universitätsstraße 25, Bielefeld 33615, Germany*

[5)] *Department of Electronic & Electrical Engineering, UCL, London WC1E 7JE, UK*

I. ADDITIONAL EXPERIMENTAL DETAILS

A. Additional Probehead Details

The probehead was cooled down using liquid helium in a continuous flow Oxford Instruments CF935 cryostat. The temperature of the HEMT preamplifier was measured using a Lakeshore Cernox® CX-1050 resistance thermometer, while the sample temperature was inferred from the inbuilt cryostat sensor. To ensure proper thermalization of the microwave components, all experiments were performed once sample and preamplifier temperatures equalized.

B. Benchmarking SNR Improvement

We characterised the SNR improvement from our new probehead in pulsed EPR at different sample/HEMT temperatures using a standard coal sample in a 4 mm outer diameter EPR tube, applying a Hahn echo pulse sequence ($\pi/2 - \tau - \pi - \tau -$ echo) with two-step phase cycling. For measurements using a 6 dB directional coupler, the duration of the $\pi/2$- and π-pulses was $t_{\pi/2} = 20$ and $t_\pi = 40$ ns, respectively, with the resonator overcoupled to a quality factor of ∼150. Given the large intrinsic signal from this test sample, the interpulse delay τ was adjusted to produce a sufficiently weak echo signal to avoid saturation of the digitizer and microwave amplifier in the bridge ($\tau = 1.5$ µs at room temperature and 4 µs at 6 K). The effects of strongly suppressed room-temperature noise were investigated at 6 K using a 30 dB directional coupler, but this required increasing the pulse durations to $t_{\pi/2} = 100$ and $t_\pi = 200$ ns with a resonator quality factor of ∼350. For this experiment, the interpulse delay τ was set to 4.5 µs.

The improved SNR with the preamplifier was benchmarked against a standard reflection setup obtained by bypassing the directional coupler in Fig. 1 and directly connecting the input microwave line to the resonator. The resonator coupling arm and sample position were tightly fixed to avoid potential variations during the switching between both setups.

[a)] Electronic mail: m.simenas@ucl.ac.uk
[b)] Electronic mail: jjl.morton@ucl.ac.uk

All parameters, except for the microwave power and negligible changes in the microwave frequency and magnetic field, were kept constant in both measurements. The microwave power was adjusted to yield the same duration of the π-pulse in both cases, and the field position was verified by an EDFS obtained using the same pulse sequence.

In determining the SNR, the Hahn echo traces were corrected by subtracting constant backgrounds that proved to be almost negligible, and the spin signal intensity was taken as a maximum of an echo obtained by fitting a Gaussian peak function. The noise was calculated as the standard deviation of the signal far away from the echo. At least 500 points were used to calculate the noise, and at least 8 separate measurements of each echo trace were performed allowing us to estimate an uncertainty in the SNR figure.

We also observed SNR improvements of CW EPR at 50 K using our probehead. For these measurements, we used a powder sample of $[(CH_3)_2NH_2][Zn(HCOO)_3]$ metal-organic framework, where 1 mol% of Zn(II) was replaced by Cu(II) (see Ref. 1 for more details). The experiments were performed using 0.5 G and 100 kHz modulation of the external field, while the microwave power reaching the resonator was set to 0.2 µW. The resonator quality factor of 3300 and sample position were fixed in both cases. At least 8 measurements of each spectrum were performed to calculate the SNR improvement and its uncertainty.

C. HYSCORE

For HYSCORE measurements, we used a *Bos Taurus* respiratory complex I sample. NADH: ubiquinone oxidoreductase (complex I) was purified from *Bos Taurus* mitochondria using an optimized protocol first described by Sharpley *et al.*[2]. The complex I sample at 30 µM concentration was prepared in a temperature independent pH 6.0 buffer[3]. The reduction potential was adjusted to −167 mV with respect to a standard hydrogen electrode using the method described in Ref. 4 before being flash frozen in a Q-band EPR tube (2 mm outer diameter, sample volume 9 µl). During the experiments, the Q-band tube was placed inside an X-band tube of 4 mm outer diameter. A more detailed description of the sample preparation is given in Ref. 3.

HYSCORE experiments were performed using the four-pulse sequence ($\pi/2 - \tau - \pi/2 - t_1 - \pi - t_2 - \pi/2 - \tau -$ echo) with four-step phase cycling[5]. Pulse durations were $t_{\pi/2} = 16$ and $t_\pi = 28$ ns, and depending on whether suppression of the matrix protons was desired, τ was set to 262 ns (suppression) or 296 ns (no suppression). The delays t_1 and t_2 were incremented from 100 to 2484 ns in steps of 16 ns. HYSCORE spectra were obtained by the fast Fourier transform (FFT) of the time domain signal after background correction, Hamming apodization and zero filling. Experiments were performed at 10 K using a shot repetition time of 2 ms. The same parameters of the pulse sequence and number of averages were used for measurements on both setups. For each measurement, the magnetic field was adjusted to a maximum in the EDFS spectrum, which corresponds to the $g_\perp$ position of the powder pattern. The resonator coupling was kept fixed, and the quality factor was about 150. The SNR was estimated by taking the ratio of the spin signal intensity and standard deviation of noise away from the signal.

D. DEER

For dipolar spectroscopy experiments, we used nitroxide and Cu(II) rulers (see Fig. S6)[6–10]. The nitroxide ruler (expected mean distance $r_{\text{NO-NO}} = 4.2$ nm) was diluted to approximately 40 µM in deuterated ortho-terphenyl (dOTP), and the Cu(II) ruler (expected mean distance $r_{\text{Cu-Cu}} = 4.5$ nm) was diluted to 200 µM in a 1:1 (v:v) mixture of D_2O/d_8-glycerol. Approximately 35 µl of samples were transferred to 3 mm outer diameter NewEra quartz capillaries and flash frozen from the liquid state (ensured for the dOTP sample by heating to 70°C) by immersion in liquid nitrogen.

We used the four-pulse DEER sequence[11] with fixed (detection) refocusing delays set to

$d_1 = 400$ ns and $d_2 = 8$ µs. The pump pulse was set to 40 ns, while other pulses had a duration of 32 ns. The initial delay of the inversion pulse after the first refocusing pulse was 280 ns, which was then incremented in steps of 16 ns for a total of 450 points. We did not use orientation averaging or nuclear modulation averaging protocols, as these procedures are not required for comparing sensitivity of different setups. Spectral separation of the pump and detection frequency was 60 MHz for both samples. The detection and pump frequencies were approximately equidistant from the center of the resonator, which was overcoupled to a quality factor of approximately 150. The experiments were performed at 50 and 10 K for the nitroxide and Cu(II) ruler, respectively, with corresponding shot repetition time of 3 and 15 ms. The same parameters including the resonator coupling and number of averages were used for the same ruler on both setups.

Data analysis was performed with DeerAnalysis2019[12]. All DEER traces were truncated at $t_{\max} = 6$ µs to exclude terminal artifacts. The background dimensionality was allowed to vary during the fitting. The form factors were obtained by background division, and the resulting traces were fitted with Tikhonov regularization using the AIC criterion[13] for optimal selection of the regularization parameter α. The fitted distance distributions were validated using all available criteria in DeerAnalysis2019 (white noise, background start, background dimensionality, background density, and modulation depth) in a rough grid, resulting in 21780 evaluations (with the optimal α) per trace. The fitted distance distributions from the Cu(II)-Cu(II) DEER measurements were corrected to account for the effective g-factors of the pumped and detected spins ($g_p = 2.048$, $g_d = 2.060$) by applying a correction factor to the distance axis $R' = Rg_pg_d/g_e^2$, where g_e is the free electron g-factor[14]. The SNR improvement was estimated by taking the ratio of the noise levels for both setups, where noise was obtained as a standard deviation from the fit residuals.

E. Note on Eq. (3)

By taking into account the noise temperature of the HEMT (T_{H}) and the microwave amplifier in the bridge (T_{B}), the equation for the SNR improvement can be expressed as

$$\frac{\mathrm{SNR_H}}{\mathrm{SNR_0}} = \sqrt{\frac{290\ [\mathrm{K}] + T_{\mathrm{B}}}{T_{\mathrm{S}} + T_{\mathrm{H}}}}\frac{L_{\mathrm{RB}}}{L_{\mathrm{RH}}}, \tag{S1}$$

The noise temperature of the HEMT is substantially lower than the sample temperature T_{S} in the whole investigated temperature range and therefore it is neglected in our analysis. The resulting equation can be expressed as

$$\frac{\mathrm{SNR_H}}{\mathrm{SNR_0}} = \sqrt{\frac{290\ [\mathrm{K}]}{T_{\mathrm{S}}}}\sqrt{1 + \frac{T_{\mathrm{B}}}{290\ [\mathrm{K}]}}\frac{L_{\mathrm{RB}}}{L_{\mathrm{RH}}}. \tag{S2}$$

By including the factor containing T_{B} into L_{RB}, the equation used in the main text is recovered:

$$\frac{\mathrm{SNR_H}}{\mathrm{SNR_0}} = \sqrt{\frac{290\ [\mathrm{K}]}{T_{\mathrm{S}}}}\frac{L_{\mathrm{RB}}}{L_{\mathrm{RH}}}. \tag{S3}$$

In this form, the factor L_{RB} takes into account the SNR degradation due to a non-negligible noise temperature of the amplifier in the microwave bridge.

F. Noise Figure Measurements

We used a vector network analyzer (VNA) to measure the microwave losses in the detection circuits of both spectrometers (I and II) employed to benchmark the SNR improvement at different temperature. Transmission measurements performed from the resonator to the microwave amplifier in the bridge revealed microwave attenuation of 7.5 dB (I) and 6.3 dB (II). The difference of 1.2 dB is not sufficient to fully account for the observed 3 dB difference in L_{RB}. The remaining discrepancy may originate from the differences in the performance of the microwave amplifiers. However, the specifications of these amplifiers are unknown to us. We also cannot reject a possibility that the microwave amplifier in the first spectrometer is slightly damaged.

We expect that a properly working amplifier in the Bruker bridge has a noise figure of about 2 dB at room temperature. Thus, the total measured noise figure of the second spectrometer (including the probehead) would be about 8-9 dB, which is rather close to $L_{\mathrm{RB}} = 10$ dB determined from the temperature-dependent measurements. The remaining discrepancy likely originates from the simplified noise analysis, which does not include the resonator coupling effects and temperature dependent losses of the microwave components and the noise temperature of the HEMT.

G. Room-temperature Noise Source

We investigated a possible origin of room-temperature noise reaching the sample. We observed the same noise level using Bruker spectrometer when the TWT output is replaced with a 50 Ω load on the circulator in the microwave bridge. The same noise level was also observed for connected TWT regardless of the attenuation of the pulses. This suggests that TWT acts as a room temperature noise source.

References

[1] M. Šimėnas, A. Ciupa, G. Usevicius, K. Aidas, D. Klose, G. Jeschke, M. Maczka, G. Völkel, A. Pöppl, J. Banys, Electron paramagnetic resonance of a copper doped $[(CH_3)_2NH_2][Zn(HCOO)_3]$ hybrid perovskite framework, Phys. Chem. Chem. Phys. 20 (2018) 12097–12105.

[2] M. S. Sharpley, R. J. Shannon, F. Draghi, J. Hirst, Interactions between Phospholipids and NADH:Ubiquinone Oxidoreductase (Complex I) from Bovine Mitochondria, Biochemistry 45 (2006) 241–248.

[3] N. Le Breton, J. J. Wright, A. J. Y. Jones, E. Salvadori, H. R. Bridges, J. Hirst, M. M. Roessler, Using hyperfine electron paramagnetic resonance spectroscopy to define the proton-coupled electron transfer reaction at Fe-S cluster N_2 in respiratory complex I, J. Am. Chem. Soc. 139 (2017) 16319–16326.

[4] J. J. Wright, E. Salvadori, H. R. Bridges, J. Hirst, M. M. Roessler, Small-volume potentiometric titrations: EPR investigations of Fe-S cluster N_2 in mitochondrial complex I, J. Inorg. Biochem. 162 (2016) 201–206.

[5] P. Höfer, A. Grupp, H. Nebenführ, M. Mehring, Hyperfine sublevel correlation (hyscore) spectroscopy: a 2D ESR investigation of the squaric acid radical, Chem. Phys. Lett. 132 (1986) 279–282.

[6] G. Jeschke, M. Sajid, M. Schulte, N. Ramezanian, A. Volkov, H. Zimmermann, A. Godt, Flexibility of shape-persistent molecular building blocks composed of p-phenylene and ethynylene units, J. Am. Chem. Soc. 132 (2010) 10107–10117.

[7] M. Qi, M. Hülsmann, A. Godt, Spacers for geometrically well-defined water-soluble molecular rulers and their application, J. Org. Chem. 81 (2016) 2549–2571.

[8] M. Qi, M. Hülsmann, A. Godt, Synthesis and hydrolysis of 4-Chloro-PyMTA and 4-Iodo-PyMTA esters and their oxidative degradation with Cu(I/II) and oxygen, Synthesis 48 (2016) 3773–3784.

[9] R. Tschaggelar, F. D. Breitgoff, O. Oberhänsli, M. Qi, A. Godt, G. Jeschke, High-bandwidth Q-band EPR resonators, Appl. Magn. Reson. 48 (2017) 1273–1300.

[10] K. Keller, I. Ritsch, H. Hintz, M. Hülsmann, M. Qi, F. Breitgoff, D. Klose, Y. Polyhach, M. Yulikov, A. Godt, G. Jeschke, Accessing distributions of exchange and dipolar couplings in stiff molecular rulers with Cu(II) centres (2020). Submitted.

[11] M. Pannier, S. Veit, A. Godt, G. Jeschke, H. Spiess, Dead-time free measurement of dipole-dipole interactions between electron spins, J. Magn. Reson. 142 (2000) 331–340.

[12] G. Jeschke, V. Chechik, P. Ionita, A. Godt, H. Zimmermann, J. Banham, C. R. Timmel, D. Hilger, H. Jung, DeerAnalysis2006 - a comprehensive software package for analyzing pulsed ELDOR data, Appl. Magn. Reson. 30 (2006) 473–498.
[13] T. H. Edwards, S. Stoll, Optimal Tikhonov regularization for DEER spectroscopy, J. Magn. Reson. 288 (2018) 58–68.
[14] F. D. Breitgoff, K. Keller, M. Qi, D. Klose, M. Yulikov, A. Godt, G. Jeschke, UWB DEER and RIDME distance measurements in Cu(II)-Cu(II) spin pairs, J. Magn. Reson. 308 (2019) 106560.

II. SUPPLEMENTARY FIGURES

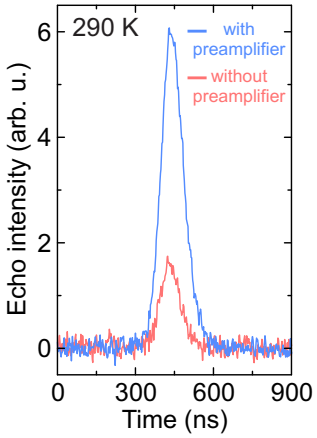

FIG. S1. Hahn echoes of the coal sample obtained at 290 K using a setup with and without the preamplifier. Signals are normalized to the noise level. Experimental parameters: $\tau = 1.5$ µs, 600 averages and $t_\pi = 40$ ns. Each measurement was performed at a magnetic field, which corresponds to the maximum of the EDFS spectrum.

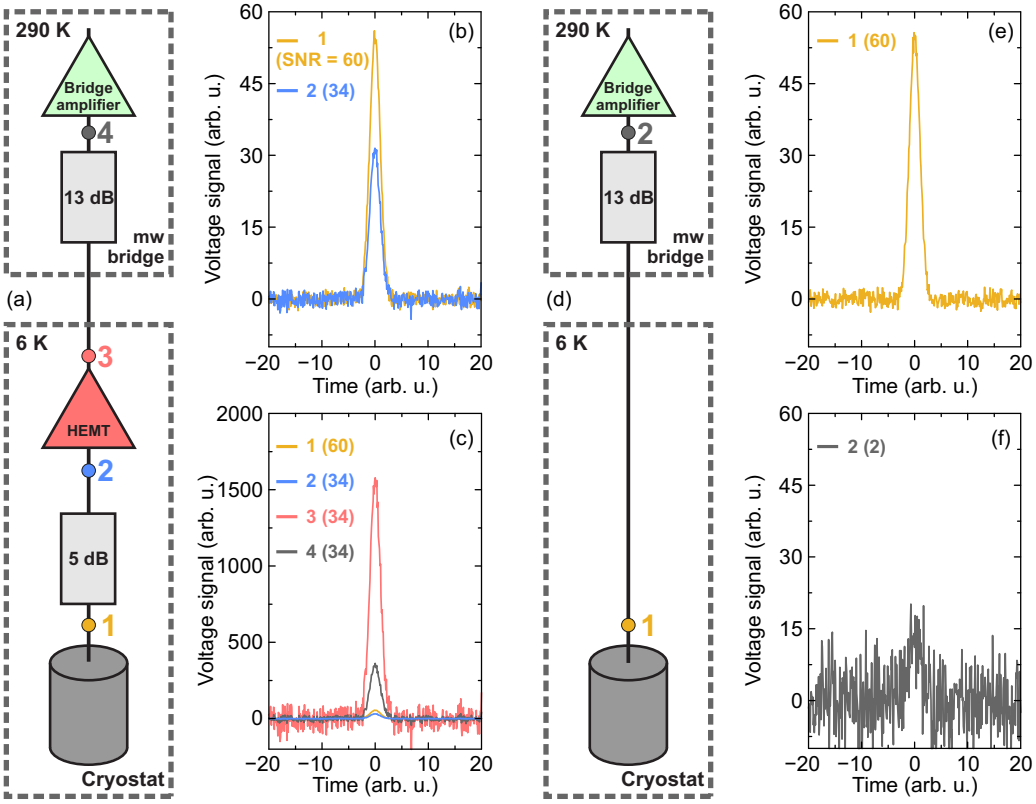

FIG. S2. Schematic propagation of the spin signal and noise in the (a) HEMT and (d) standard setups. The corresponding signal and noise together with the values of SNR at different stages of both setups are presented in (b)-(c) and (e)-(f). The spin signal was simulated as a Gaussian function to which random noise was added with initial noise power at stage 1 corresponding to 6 K. It is assumed that each lossy component attenuates both signal and noise, also adding additional noise with noise power corresponding to temperature. The gain of the preamplifier in (a) is 34 dB.

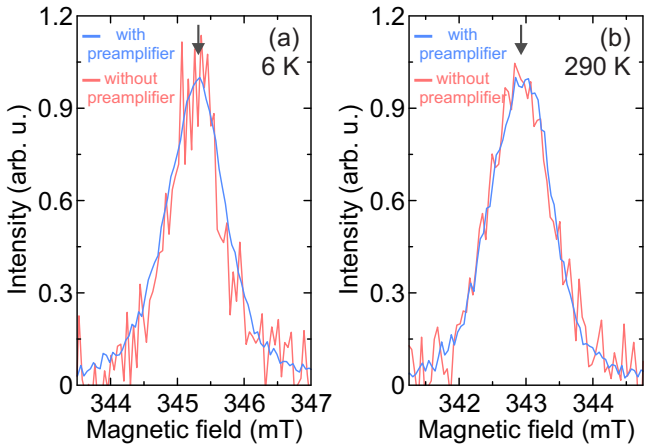

FIG. S3. Normalized EDFS spectra of the coal sample obtained at (a) 6 and (b) 290 K using a setup with and without the preamplifier. Experimental parameters: (a) $\tau = 4$ µs, 1 average, $t_\pi = 40$ ns and (b) $\tau = 1.5$ µs, 50 averages, $t_\pi = 40$ ns. The arrows indicate the fields, at which the Hahn echo experiments were performed.

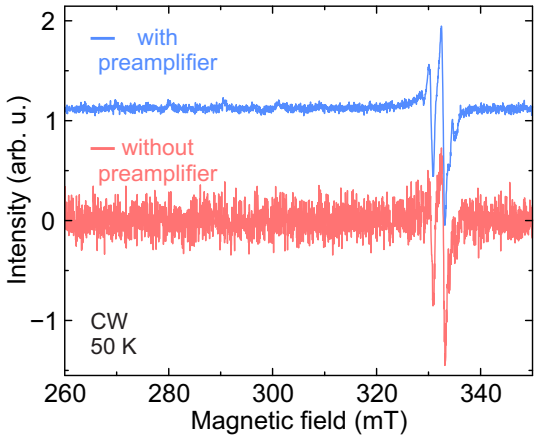

FIG. S4. CW EPR spectra of Cu(II) ions in $[(CH_3)_2NH_2][Zn(HCOO)_3]$ obtained at 50 K using a setup with and without the preamplifier. Measurements with the preamplifier were performed using a 6 dB directional coupler. Spectra are normalized to the Cu(II) signal.

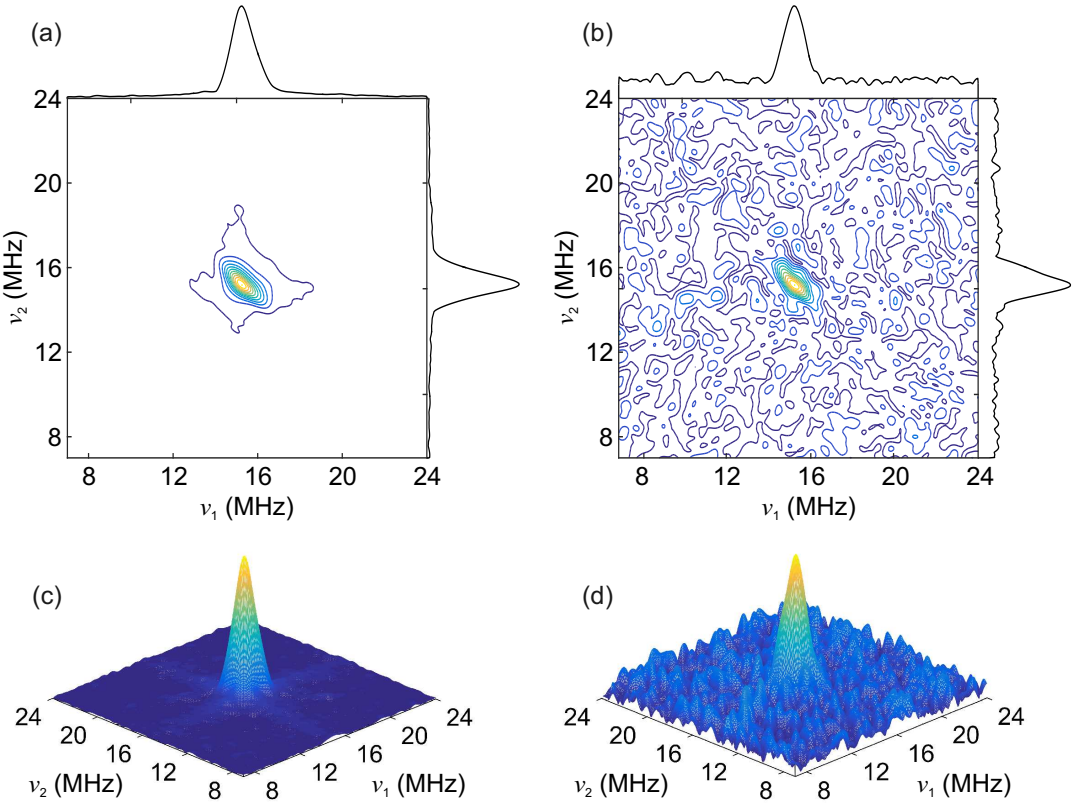

FIG. S5. Contour plots with the skyline projections of the ^{1}H HYSCORE spectra of *Bos Taurus* complex I measured using (a) HEMT and (b) standard setups. The corresponding 3D plots are presented in (c) and (d). Spectra were obtained at 10 K and 357.7 mT using $\tau = 296$, $t_{\pi/2} = 16$, $t_\pi = 28$ ns and an acquisition time of 1.5 hours.

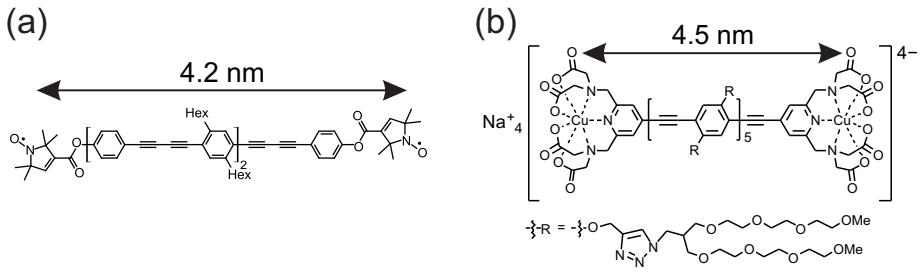

FIG. S6. Structures of (a) nitroxide and (b) Cu(II) rulers used for the DEER experiments.

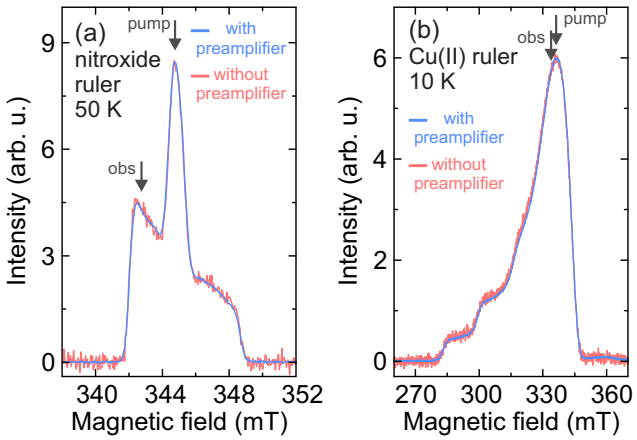

FIG. S7. Normalized EDFS spectra of the (a) nitroxide and (b) Cu(II) ruler samples obtained using a setup with and without the preamplifier. Experimental parameters: (a) $\tau = 400$ ns, 10 averages, $t_\pi = 40$ ns, 50 K and (b) $\tau = 400$ ns, 10 averages, $t_\pi = 32$ ns, 10 K. The arrows indicate pump and observer field positions used for the DEER experiments.

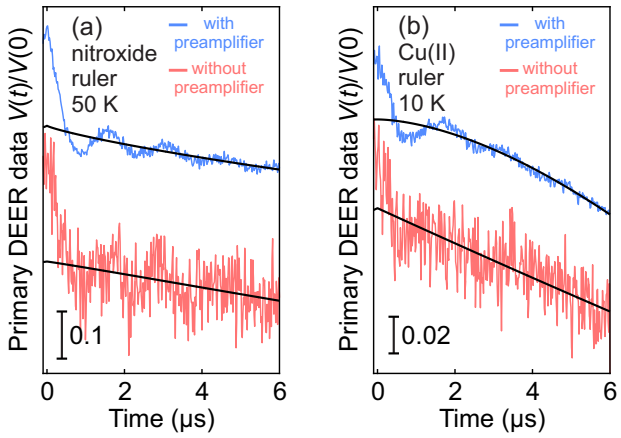

FIG. S8. Primary DEER data of (a) nitroxide and (b) Cu(II) rulers measured using a setup with and without the preamplifier. The black curves indicate background fits.